SIAM J. APPL. MATH.
Vol. 75, No. 5, pp. 2361–2378

DYNAMIC TRANSITIONS OF QUASI-GEOSTROPHIC CHANNEL FLOW*

HENK DIJKSTRA†, TAYLAN SENGUL‡, JIE SHEN§, AND SHOUHONG WANG¶

Abstract. The main aim of this paper is to study the dynamic transitions in flows described by the two-dimensional, barotropic vorticity equation in a periodic zonal channel. In [Z.-M. Chen et al., *SIAM J. Appl. Math.*, 64 (2003), pp. 343–368], the existence of a Hopf bifurcation in this model as the Reynolds number crosses a critical value was proven. In this paper, we extend these results by addressing the stability problem of the bifurcated periodic solutions. Our main result is the explicit expression of a nondimensional parameter γ which controls the transition behavior. We prove that depending on γ, the modeled flow exhibits either a continuous (Type I) or catastrophic (Type II) transition. Numerical evaluation of γ for a physically realistic region of parameter space suggests that a catastrophic transition is preferred in this flow, which may lead to chaotic flow regimes.

Key words. quasi-geostrophic flow, channel flow, spatial-temporal patterns, dynamic transitions, climate variability

AMS subject classifications. 35Q30, 76E20, 35B35, 37G15, 86A10

DOI. 10.1137/15M1008166

1. Introduction.

Climate variability exhibits recurrent large-scale patterns that are directly linked to dynamical processes represented in the governing dissipative dynamical system [6, 7, 8]. The study of the persistence of these patterns and the transitions between them also plays a crucial role in understanding climate change and in interpreting future climate projections [9].

Current climate models used for developing such projections are based on the conservation laws of fluid mechanics and consist of systems of nonlinear partial differential equations (PDEs). These models can be put into the perspective of infinite-dimensional nonlinear dissipative systems exhibiting large-dimensional attractors. The global attractor is a mathematical object strongly connected to the overall dissipation in the system. Climate variability is, however, often associated with dynamic transitions between different regimes, each represented by local attractors.

There are many examples of climate phenomena where such transitions have been investigated numerically, such as the transition to oscillatory behavior in models of the El Niño/Southern Oscillation phenomenon in the equatorial Pacific, the transitions between different mean flow patterns of the Kuroshio Current in the North Pacific, and the transitions between blocked and zonal flows in the midlatitude atmosphere

*Received by the editors February 12, 2015; accepted for publication (in revised form) August 10, 2015; published electronically October 22, 2015.
http://www.siam.org/journals/siap/75-5/M100816.html

†Department of Physics and Astronomy, Institute for Marine and Atmospheric research Utrecht, Utrecht University, 3584 CC Utrecht, The Netherlands (H.A.Dijkstra@uu.nl). This author's research was supported by the Netherlands Organization for Scientific Research (NWO) through the COMPLEXITY project PreKurs.

‡Department of Mathematics, Marmara University, 34722, Istanbul, Turkey (taylan.sengul@marmara.edu.tr). This author's research was supported by the Scientific and Technological Research Council of Turkey (grant 114C142).

§Department of Mathematics, Purdue University, West Lafayette, IN 47907 (shen7@purdue.edu). This author's research was partially supported by NSF grants DMS-1217066 and DMS-1419053.

¶Department of Mathematics, Indiana University, Bloomington, IN 47405 (showang@indiana.edu, http://www.indiana.edu/∼fluid). This author's research was supported in part by NSF grants DMS-1211218 and DMS-1515024, and by ONR grant N00014-15-1-2662.

(see, e.g., [5]). However, rigorous mathematical results on the type of transitions in these systems of PDEs are extremely scarce.

This paper arises out of a research program to generate rigorous mathematical results on climate variability developed from the viewpoint of dynamical transitions. The dynamic transition theory is developed in [10, 11]. The basic philosophy of dynamic transition theory is to search for the full set of transition states, giving a complete characterization of stability and transition. The set of transition states is represented by a local attractor near or away from the basic state. Following this approach, dynamic transition theory is developed to identify the transition states and to classify them both dynamically and physically. In particular, we obtained a general principle that dynamic transitions of all dissipative systems are classified into three categories: continuous, catastrophic, and random. These transitions are also called Type-I, Type-II, and Type-III transitions, respectively. Basically, as the control parameter passes the critical threshold, the transition states stay in a close neighborhood of the basic state for a continuous (Type-I) transition, and they are outside of a neighborhood of the basic state for a catastrophic (Type-II) transition. For the the random (Type-III) transition, a neighborhood is divided into two open regions with a continuous transition in one region and a catastrophic transition in the other region.

The main focus of this paper is on the dynamic transitions in flows described by one of the cornerstone dynamical models in both oceanic and atmospheric dynamics, the two-dimensional, dimensionless barotropic vorticity equation given by

$$\frac{\partial \Delta\psi}{\partial t} + \epsilon J(\psi, \Delta\psi) + \frac{\partial \psi}{\partial x} = E\Delta^2\psi + \alpha_\tau \sin \pi y, \tag{1.1}$$

where Δ is the Laplacian operator, $J(f, g) = (\partial f/\partial x)(\partial g/\partial y) - (\partial f/\partial y)(\partial g/\partial x)$ is the advection operator, and ψ is the geostrophic stream function. Equation (1.1) describes flows with a typical length scale L on a midlatitude beta plane with a central latitude θ_0 and a planetary vorticity gradient β_0. It can be derived from the primitive equations by the so-called quasi-geostrophic (QG) approximation, which assumes a dominant balance between the Coriolis force and the pressure gradient force [12].

To derive (1.1), time, length, and the stream function were nondimensionalized with $1/(\beta_0 L)$, L, and UL, where U is a characteristic horizontal velocity. The positive parameters ϵ and E are Rossby and Ekman numbers, respectively, given by

$$\epsilon = \frac{U}{\beta_0 L^2}, \qquad E = \frac{A_H}{\beta_0 L^3},$$

where A_H is the lateral friction coefficient. The Reynolds number R is defined as

$$R = \frac{\epsilon}{E} = \frac{UL}{A_H}. \tag{1.2}$$

The forcing term $\alpha_\tau \sin \pi y$ in (1.1) may represent the transfer of angular momentum into midlatitudes due to the tropical Hadley cell in an atmospheric model. In this case, the magnitude of the velocity can be scaled such that $\alpha_\tau = 1$. In the ocean case, the forcing term represents the dimensionless wind stress

$$\tau = \frac{\alpha_\tau}{\pi}(\cos \pi y, 0).$$

Such a wind stress mimics the annually averaged zonal wind distribution over the North Atlantic and North Pacific with westerly (i.e., eastward) winds over the midlatitudes and easterlies in the tropics and polar latitudes. When the dimensionless

wind stress has a magnitude τ_0 and the ocean basin a depth D and the water a density ρ, the factor α_τ is given by

$$\alpha_\tau = \frac{\tau_0}{\rho D L \beta_0 U}.$$

In this case, we can choose U such that $\alpha_\tau = 1$, which is usually referred to as the Sverdrup scaling. In both the ocean and the atmosphere cases, (1.1) has two free parameters (out of the three ϵ, E, and R) which we choose here as R and E.

We consider flows in a so-called zonal channel of length $2/a$ with walls bounding the domain at $y = \pm 1$ and periodic conditions in the zonal direction. Equation (1.1) is therefore supplemented with boundary conditions

$$\begin{aligned} &\psi\,|_{x=0} = \psi\,|_{x=2/a}, \\ &\psi\,|_{y=\pm 1} = \frac{\partial^2 \psi}{\partial y^2}\,|_{y=\pm 1} = 0. \end{aligned} \tag{1.3}$$

Equation (1.1) together with (1.3) admits the following steady state:

$$\psi_0 = -\frac{1}{\pi^4 E} \sin \pi y, \tag{1.4}$$

which represents a zonal jet with zonal velocity field $u_0 = -\partial \psi_0 / \partial y = 1/(\pi^3 E) \cos \pi y$.

It is shown in [3] that for any $a \geq \sqrt{3}/2$, ψ_0 is both linearly and nonlinearly stable. Also, there is an α_0 with $\sqrt{3}/4 < \alpha_0 < \sqrt{3}/2$ such that for any $\sqrt{3}/4 \leq a \leq \alpha_0$ there is a critical Reynolds number $R_0 > 0$ depending on a such that a simple pair of complex conjugate eigenvalues crosses the imaginary axis as the Reynolds number R crosses R_0, leading to the existence of Hopf bifurcation at the critical Reynolds number. However, the stability of the bifurcated periodic solutions and the dynamic transition behavior near R_0 are so far unknown. The main difficulty is caused by the lack of an explicit analytical form of the eigenfunctions.

The main objective of this paper is to investigate the dynamic transition and the stability of the basic state (1.4) as the Reynolds number crosses a critical threshold R_0. The main result of this paper is that the dynamic transition from this state to new states is either continuous (Type-I) or catastrophic (Type-II) and is determined by the sign of a computable parameter γ given by (2.10). Our numerical investigations indicate that in a physically relevant parameter regime, only catastrophic transitions occur.

More precisely, the key ingredient of the study is to capture the nonlinear interactions of different modes, including the self- and cross-interactions of both stable modes and unstable modes. In fact, a nondimensional computable parameter γ is derived, accounting for the precise interactions of these modes. The main difficulties are two-fold. First, as mentioned earlier, the linear eigenvalue problem of the underlying problem is not separable, and there is no simple analytical form of the associated eigenmodes. Second, the lack of an explicit analytical form of the eigenmodes leads also to an additional difficulty for deriving the detailed information for the nonlinear interactions of different modes. To overcome these difficulties, in this paper, we initiate a study by combining rigorous analysis with numerical computation. The study addresses the nonlinear interactions of different modes and the reduction of the original PDE system to a finite-dimensional dynamical system dictated by the unstable modes and their nonlinear interactions with the infinite-dimensional stable modes.

For the physical problem studied in this paper, first we show that the dynamical behavior is completely dictated by the sign of the parameter $\gamma = \gamma(a, \epsilon, E)$, which depends on the physical parameters of the system: the length scale a, the Rossby number ϵ, and the Ekman number E. In particular, the parameter equation

$$\gamma(a, \epsilon, E) = 0 \tag{1.5}$$

gives rise to the phase transition diagram in terms of the related physical parameters. Then a computational approach based on the spectral method is established to compute the eigenmodes of the linearized problem, their nonlinear interactions, and the resulting parameter γ, leading to detailed information on the transition behavior of the underlying physical problem.

2. Main theorem. Throughout, $\operatorname{Re} z$, $\operatorname{Im} z$, and $\overline{z}$ will denote the real part, the imaginary part, and the complex conjugate of a complex number z. $D = \frac{d}{dy}$ is the derivative operator, $\Omega = (0, 2/a) \times (-1, 1)$ is a rectangular box in $\mathbb{R}^2$, and $(\cdot, \cdot)$ is the $L^2(\Omega)$ inner product.

2.1. Functional setting. Considering the deviation $\psi' = \psi - \psi_0$ from the basic steady state (1.4) and omitting the primes, we obtain from (1.1)

$$\frac{\partial \Delta\psi}{\partial t} + \epsilon J(\psi, \Delta\psi) = -\frac{R}{\pi^3} \cos \pi y \left[\Delta \frac{\partial \psi}{\partial x} + \pi^2 \frac{\partial \psi}{\partial x} \right] - \frac{\partial \psi}{\partial x} + E\Delta^2 \psi. \tag{2.1}$$

Note that (1.1) can also be formulated in velocity $\mathbf{u} = (-\frac{\partial \psi}{\partial y}, \frac{\partial \psi}{\partial x})$ and pressure p as

$$\begin{aligned} &\frac{\partial \mathbf{u}}{\partial t} + \epsilon(\mathbf{u} \cdot \nabla)\mathbf{u} + f\mathbf{k} \times \mathbf{u} = E\Delta\mathbf{u} - \nabla p + \tau, \\ &\nabla \cdot \mathbf{u} = 0. \end{aligned} \tag{2.2}$$

Here f is the dimensionless Coriolis parameter on a midlatitude beta plane that gives rise to the $\partial\psi/\partial x$ term in (1.1), and $\mathbf{k}$ is the unit vector in the z-direction.

Using the formulation (2.2), we can write the problem in the following abstract form:

$$\frac{d\mathbf{u}}{dt} = L\mathbf{u} + G(\mathbf{u}), \tag{2.3}$$

where $L : H_1 \to H$ is the linear operator, $G : H_1 \to H$ is the nonlinear operator, and

$$\begin{aligned} H &= \{\mathbf{u} = (u, v) \in (L^2(\Omega))^2 \mid \quad v \mid_{y=\pm 1} = 0, \operatorname{div}\mathbf{u} = 0, \mathbf{u} \mid_{x=0} = \mathbf{u} \mid_{x=2/a}\}, \\ H_1 &= H \cap (H^1(\Omega))^2. \end{aligned}$$

Also, we use $P : L^2(\Omega)^2 \to H$ to stand for the Leray projection.

As mentioned in the introduction, the main objective of this paper is to study the dynamic transition behavior of the basic state ψ_0, or equivalently the dynamic transition behavior near $\psi = 0$ for the deviation equation (2.3). The analysis is carried in the following steps. First, a linear analysis of the eigenvalue problem associated with (2.3) is needed to identify the unstable modes, leading to both linear and nonlinear instabilities and the nonlinear transitions. Second, we derive detailed characterizations of the nonlinear interactions of both stable and unstable modes and obtain low-dimensional center manifold reductions of the original system. Third, the

dynamical transition behavior is then fully characterized using the reduced model, representing the true dynamical transition behavior of the original system.

The eigenvalue problem for the linear operator L reads as

$$E\Delta^2\psi + \frac{R}{\pi^3}\cos(\pi y)(\Delta\psi_x + \pi^2\psi_x) - \psi_x = \beta\Delta\psi, \tag{2.4}$$

supplemented with boundary conditions (1.3).

Since the solution ψ is periodic in x with period $2/a$, we expand ψ in Fourier series, and for the m-mode of the expansion we write

$$\psi = e^{i\alpha_m x}Y(y), \quad \alpha_m = am\pi, \tag{2.5}$$

where $Y(y)$ satisfies the boundary condition $Y(\pm 1) = D^2Y(\pm 1) = 0$. Plugging (2.5) into (2.4), we obtain a sequence of one-dimensional problems

$$E(D^2 - \alpha_m^2)^2 Y + i\alpha_m\left(\frac{R}{\pi^3}\cos(\pi y)(D^2 - \alpha_m^2 + \pi^2) - 1\right)Y = \beta(D^2 - \alpha_m^2)Y. \tag{2.6}$$

The eigenvectors of (2.4) are

$$\psi_{m,j} = e^{i\alpha_m x}Y_{m,j}(y) \quad \text{for } m \in \mathbb{Z}, j = 1, 2, 3, \ldots,$$

where $Y_{m,j}$ are the eigenvectors of (2.6) corresponding to the eigenvalues $\beta_{m,j} \in \mathbb{C}$. Moreover, $\beta_{m,j}$ can be ordered so that $\operatorname{Re}\beta_{m,j} \le \operatorname{Re}\beta_{m,k}$ if $j > k$. Also, $\beta_{-m,j} = \overline{\beta_{m,j}}$ and we can take $\psi_{-m,j} = \overline{\psi_{m,j}}$. In particular, $\psi_{0,j}$ and $\beta_{0,j}$ are real.

We also need to consider the eigenvalue problem for the adjoint linear operator, which can be written as

$$E\Delta^2\psi^* - \frac{R}{\pi^3}\Delta(\cos(\pi y)\psi_x^*) - \frac{R}{\pi^3}\pi^2\cos(\pi y)\psi_x^* + \psi_x^* = \beta\Delta\psi^*.$$

Using $\psi^* = e^{i\alpha_m x}Y^*(y)$, we obtain the analogue of (2.6):

$$\begin{aligned} E(D^2 - \alpha_m^2)^2 Y^* - i\alpha_m\left(\frac{R}{\pi^3}D^2(Y^*\cos(\pi y)) + \frac{R}{\pi^3}\cos(\pi y)(\pi^2 - \alpha_m^2)Y^* - Y^*\right) \\ = \beta^*(D^2 - \alpha_m^2)Y^*. \end{aligned} \tag{2.7}$$

By basic properties of the adjoint linear eigenvalue problem, we have $\beta_{m,j}^* = \overline{\beta_{m,j}}$ and

$$(\mathbf{u}_{m,j}, \mathbf{u}_{n,k}^*) = 0 \quad \text{if } (m,j) \ne (n,k), \tag{2.8}$$

where $\mathbf{u}_{m,j} = (\frac{\partial}{\partial y}, -\frac{\partial}{\partial x})\psi_{m,j}$.

2.2. The main theorem and its proof. Our main aim is to identify the nonlinear transitions of (2.1) in the case where two complex conjugate eigenvalues cross the imaginary axis. Thus, we assume the following condition on the spectrum of the linearized operator.

Assumption 1. Depending on a and E, there exist a critical Reynolds number R_0 and a zonal wave integer $m_0 \ge 1$ such that

$$\operatorname{Re}(\beta_{m_0,1}(R)) = \operatorname{Re}(\beta_{-m_0,1}(R)) = \begin{cases} < 0 & \text{if } R < R_0, \\ = 0 & \text{if } R = R_0, \\ > 0 & \text{if } R > R_0, \end{cases}$$

$$\operatorname{Re}(\beta_{m,j}(R_0)) < 0 \quad \text{if } (m,j) \ne (\pm m_0, 1).$$

In [3], the validity of Assumption 1 is shown with $m_0 = 1$ when $\sqrt{3}/4 \le a \le \alpha_0$ for some $\sqrt{3}/4 < \alpha_0 < \sqrt{3}/2$.

Let us define

$$
\begin{aligned}
I_1 &= \int_{-1}^{1} \overline{Y^*_{m_0,1}}(y)\left((am_0\pi)^2 - D^2\right) Y_{m_0,1}(y)dy,\\
I_2(k) &= \int_{-1}^{1} \cos(k\pi y) Y^*_{m_0,1}(y)\left((am_0\pi)^2 - k^2\pi^2 - D^2\right)\overline{Y_{m_0,1}}(y)dy,\\
I_3(k) &= \int_{-1}^{1} \sin(k\pi y) Y_{m_0,1}(y) D\overline{Y_{m_0,1}}(y)dy,
\end{aligned}
\tag{2.9}
$$

where $Y_{m_0,1}$ and $Y^*_{m_0,1}$ are solutions of (2.6) and (2.7), respectively, for $m = m_0$, at $R = R_0$.

We define the transition number

$$
\gamma = -\frac{E(R_0 a m_0)^2\pi}{2|I_1|^2}\sum_{k=1}^{\infty}\frac{\operatorname{Im} I_3(k)\operatorname{Im}(I_1 I_2(k))}{k}. \tag{2.10}
$$

The quantity γ can be considered as a measure of the net mechanical energy transfer from all modes (with zonal wavenumber 0, i.e., independent of the zonal variable) back to the basic state. The subsequent modification of the basic state will then determine whether the leading mode (with zonal wavenumber m_0) will develop into an attracting or repelling periodic orbit.

We know that as soon as the linear problem indicates an instability, the nonlinear system always undergoes a (nonlinear) dynamic transition, leading to one of the three types of transitions, continuous, catastrophic, or random, as described in the introduction; see also [11].

The type of transition is determined by the reduction of the system (2.1) to the center manifold in the first unstable eigenmodes. We refer the reader to [11] for a detailed rigorous discussion of this theory with numerous applications.

As the next theorem shows, the sign of γ determines the type of dynamic transition of the original system at the critical Reynolds number R_0. In the cases studied we show that a continuous transition gives rise to a stable bifurcated periodic solution, while a catastrophic transition gives rise to an unstable bifurcated periodic solution.

THEOREM 2.1. *Let γ be defined by* (2.10)*, and let*

$$
\mathbf{u}_{bif}(t,x,y) = \sqrt{\frac{-\operatorname{Re}(\beta_{m_0,1})}{\gamma}}\operatorname{Re}\left(e^{it\operatorname{Im}(\beta_{m_0,1})}\mathbf{u}_{m_0,1}(x,y)\right) + o\left(\sqrt{|\operatorname{Re}\beta_{m_0,1}|}\right). \tag{2.11}
$$

Under Assumption 1*, the following assertions hold true:*

1. *If $\gamma < 0$, then problem* (2.2) *undergoes a Type-*I *(continuous) transition at $R = R_0$ and bifurcates to the time periodic solution $\mathbf{u}_{bif}$ on $R > R_0$, which is an attractor.*
2. *If $\gamma > 0$, then problem* (2.2) *undergoes a Type-*II *(catastrophic) transition at $R = R_0$ and bifurcates to the time periodic solution $\mathbf{u}_{bif}$ on $R < R_0$, which is a repeller.*

Proof. As outlined earlier, the proof relies heavily on the reduction of (2.2) onto the center manifold in the direction of the first critical eigenfunctions.

Let $\mathbf{u}_{m_0,1} = (\frac{\partial}{\partial y}, -\frac{\partial}{\partial x})\psi_{m_0,1}$, where $\psi_{m_0,1} = e^{iam_0\pi x}Y_{m_0,1}(y)$, and denote the first critical eigenfunction corresponding to the eigenvalue $\beta_{m_0,1}$ in Assumption 1. For simplicity of notation, we will denote

$$\begin{aligned} \mathbf{u}^1 &= \operatorname{Re}\mathbf{u}_{m_0,1}, \quad \mathbf{u}^2 = \operatorname{Im}\mathbf{u}_{m_0,1}, \\ \psi^1 &= \operatorname{Re}\psi_{m_0,1}, \quad \psi^2 = \operatorname{Im}\psi_{m_0,1}, \\ Y^1 &= \operatorname{Re}Y_{m_0,1}, \quad Y^2 = \operatorname{Im}Y_{m_0,1}, \end{aligned} \tag{2.12}$$

where $Y_{m_0,1}$ solves (2.6).

Let $G(\mathbf{u}) = -\epsilon P[(\mathbf{u}\cdot\nabla)\mathbf{u}]$ be the nonlinear operator, where P is the Leray projection. Also, for simplicity, we denote the bilinear operator again by $G(\mathbf{u},\mathbf{v}) = -\epsilon P[(\mathbf{u}\cdot\nabla)\mathbf{v}]$ so that $G(\mathbf{u}) = G(\mathbf{u},\mathbf{u})$. In the proof we will abuse the operator G to also denote the trilinear operator

$$G(\mathbf{u},\mathbf{v},\mathbf{w}) = (G(\mathbf{u},\mathbf{v}),\mathbf{w}) = -\epsilon\int_\Omega (\mathbf{u}\cdot\nabla)\mathbf{v}\cdot\overline{\mathbf{w}}dxdy. \tag{2.13}$$

Let us also define the symmetric trilinear form

$$G_s(\mathbf{u},\mathbf{v},\mathbf{w}) = G(\mathbf{u},\mathbf{v},\mathbf{w}) + G(\mathbf{v},\mathbf{u},\mathbf{w}).$$

Step 1. *Computation of nonlinear interactions.* It is easy to see that only $(0,k)$ and $(2m_0,k)$ adjoint modes interact nonlinearly with the critical $(m_0,1)$-mode. Namely,

$$G(\mathbf{u}^i,\mathbf{u}^j,\mathbf{u}^*_{n,k}) = 0 \quad \text{if } n\neq 0, \text{ or } n\neq 2m_0,\ i,j=1,2. \tag{2.14}$$

We will first investigate these interactions. We have $\mathbf{u}_{0k} = \mathbf{u}^*_{0k} = (\frac{\partial}{\partial y}\psi_{0k},0) = (DY_{0k},0)$, where Y_{0k} is given by (2.42). In particular, $\mathbf{u}^*_{0k}$ is real. Using

$$G(\mathbf{u},\mathbf{u},\mathbf{u}^*_{0k}) = C\int_{x=0}^{2/a} e^{2iam_0\pi x}dx = 0,$$

where $C = \int_{y=-1}^{1}(\text{only } y\text{-dependent terms})dy$, we get by $\mathbf{u} = \mathbf{u}^1 + i\mathbf{u}^2$,

$$0 = G(\mathbf{u}^1,\mathbf{u}^1,\mathbf{u}^*_{0k}) - G(\mathbf{u}^2,\mathbf{u}^2,\mathbf{u}^*_{0k}) + i(G(\mathbf{u}^1,\mathbf{u}^2,\mathbf{u}^*_{0k}) + G(\mathbf{u}^2,\mathbf{u}^1,\mathbf{u}^*_{0k})). \tag{2.15}$$

Also note that

$$G(\overline{\mathbf{u}},\mathbf{u},\mathbf{u}^{*l}_{2m_0,k}) = C\int_{x=0}^{2/a} e^{-i\alpha_{m_0}x}e^{i\alpha_{m_0}x}T(\alpha_{2m_0}x)dx = 0,$$

where $C = \int_{y=-1}^{1}(\text{only } y\text{-dependent terms})dy$ and $T = \sin$ or $T = \cos$. By letting $\mathbf{u}^{*1}_{2m_0,k} = \operatorname{Re}\mathbf{u}^*_{2m_0,k}$ and $\mathbf{u}^{*2}_{2m_0,k} = \operatorname{Im}\mathbf{u}^*_{2m_0,k}$, we get for $l=1,2$,

$$0 = G(\mathbf{u}^1,\mathbf{u}^1,\mathbf{u}^{*l}_{2m_0,k}) + G(\mathbf{u}^2,\mathbf{u}^2,\mathbf{u}^{*l}_{2m_0,k}) + i(G(\mathbf{u}^1,\mathbf{u}^2,\mathbf{u}^{*l}_{2m_0,k}) - G(\mathbf{u}^2,\mathbf{u}^1,\mathbf{u}^{*l}_{2m_0,k})). \tag{2.16}$$

Let us define

$$\begin{aligned} g^{ij}_{0k} &= G(\mathbf{u}^i,\mathbf{u}^j,\mathbf{u}^*_{0k}), \\ g^{ij}_{2m_0,k} &= G(\mathbf{u}^i,\mathbf{u}^j,\mathbf{u}^*_{2m_0,k}). \end{aligned} \tag{2.17}$$

We infer then from (2.15), (2.16), and (2.17) that

$$\begin{aligned} g_{0k}^{11} &= g_{0k}^{22}, & g_{0k}^{12} &= -g_{0k}^{21}, \\ g_{2m_0,k}^{11} &= -g_{2m_0,k}^{22}, & g_{2m_0,k}^{12} &= g_{2m_0,k}^{21}. \end{aligned} \tag{2.18}$$

A lengthy but straightforward calculation shows that

$$\begin{aligned} G(\mathbf{u}^1, \mathbf{u}^1, \mathbf{u}_{2m_0,k}^{*1}) &= G(\mathbf{u}^1, \mathbf{u}^2, \mathbf{u}_{2m_0,k}^{*2}), \\ G(\mathbf{u}^1, \mathbf{u}^1, \mathbf{u}_{2m_0,k}^{*2}) &= -G(\mathbf{u}^1, \mathbf{u}^2, \mathbf{u}_{2m_0,k}^{*1}), \end{aligned}$$

which implies that

$$g_{2m_0,k}^{11} = i g_{2m_0,k}^{12}. \tag{2.19}$$

Step 2. *Approximation of the center manifold.* Next we obtain an approximation for the center manifold function Φ. Let $H = E_1 \oplus E_2$, $E_1 = \operatorname{span}\{\mathbf{u}^1, \mathbf{u}^2\}$, $E_2 = \{\mathbf{u} \in H_1 \mid (\mathbf{u}, \mathbf{u}^1) = (\mathbf{u}, \mathbf{u}^2) = 0\}$ be the orthogonal complement of E_1, $P_i : H \to E_i$ be the canonical projection, and $\mathcal{L} = L\,|_{E_2}$ be the projection of the linear operator L onto E_2. By [11], near $R = R_0$, the center manifold Φ can be approximated by the formula

$$\begin{aligned} ((-\mathcal{L})^2 + 4\operatorname{Im}(\beta)^2)(-\mathcal{L})\Phi &= ((-\mathcal{L})^2 + 2\operatorname{Im}(\beta)^2)P_2 G(x_1\mathbf{u}^1 + x_2\mathbf{u}^2) \\ &\quad + 2\operatorname{Im}(\beta)^2 P_2 G(x_1\mathbf{u}^2 - x_2\mathbf{u}^1) \\ &\quad + \operatorname{Im}(\beta)(-\mathcal{L})G(x_1\mathbf{u}^1 + x_2\mathbf{u}^2, x_2\mathbf{u}^1 - x_1\mathbf{u}^2) \\ &\quad + \operatorname{Im}(\beta)(-\mathcal{L})G(x_2\mathbf{u}^1 - x_1\mathbf{u}^2, x_1\mathbf{u}^1 + x_2\mathbf{u}^2) + o(2), \end{aligned} \tag{2.20}$$

where

$$o(2) = o(x_1^2 + x_2^2) + O(|\operatorname{Re}\beta(R)|(x_1^2 + x_2^2)).$$

Let us write

$$\Phi = \sum_J \Phi_J \mathbf{u}_J.$$

Note that for an eigenvector $\mathbf{u}_K^*$ of L^* corresponding to $\beta_K^* = \overline{\beta}_K$, by orthogonality relation (2.8), we have

$$\begin{aligned} (((-\mathcal{L})^2 + 4\operatorname{Im}(\beta)^2)(-\mathcal{L})\Phi, \mathbf{u}_K^*) &= \sum_K -\Phi_J \beta_K (\beta_K^2 + 4\operatorname{Im}(\beta)^2)(\mathbf{u}_J, \mathbf{u}_K^*) \\ &= m_K \Phi_K, \end{aligned}$$

where

$$m_K = -\beta_K(\beta_K^2 + 4\operatorname{Im}(\beta)^2)(\mathbf{u}_K, \mathbf{u}_K^*).$$

By (2.14) and the center manifold formula (2.20), we have the following approximation for the center manifold:

$$\Phi = \sum_k \Phi_{0k}\mathbf{u}_{0k} + \sum_k \Phi_{2m_0,k}\mathbf{u}_{2m_0,k} + o(2). \tag{2.21}$$

Here

$$\Phi_K = \Phi_{1,K}x_1^2 + \Phi_{2,K}x_1x_2 + \Phi_{3,K}x_2^2.$$

Using these results, the coefficients of the center manifold function can be computed as follows:

$$\begin{aligned}
\Phi_{1,K} &= m_K^{-1}\left((\beta_K^2 + 2\,\mathrm{Im}(\beta)^2)g_K^{11} + 2\,\mathrm{Im}(\beta)^2 g_K^{22} + \mathrm{Im}(\beta)\beta_K(g_K^{12} + g_K^{21})\right),\\
\Phi_{2,K} &= m_K^{-1}\left(\beta_K^2(g_K^{12} + g_K^{21}) + 2\,\mathrm{Im}(\beta)\beta_K(g_K^{22} - g_K^{11})\right),\\
\Phi_{3,K} &= m_K^{-1}\left((\beta_K^2 + 2\,\mathrm{Im}(\beta)^2)g_K^{22} + 2\,\mathrm{Im}(\beta)^2 g_K^{11} - \mathrm{Im}(\beta)\beta_K(g_K^{12} + g_K^{21})\right).
\end{aligned} \tag{2.22}$$

Using (2.18), (2.19), and (2.22), we find that

$$\Phi_{1,0k} = \Phi_{3,0k}, \qquad \Phi_{2,0k} = 0, \quad \Phi_{1,2m_0,k} = \frac{i}{2}\Phi_{2,2m_0,k} = -\Phi_{3,2m_0,k}.$$

Hence the center manifold function (2.21) becomes

$$\Phi = \sum_k \Phi_{1,0k}\mathbf{u}_{0k}(x_1^2 + x_2^2) + \Phi_{1,2m_0,k}(x_1^2 - 2ix_1x_2 - x_2^2)\mathbf{u}_{2m_0,k} + o(2). \tag{2.23}$$

Note that $\Phi_{1,0k}$ is real, while $\Phi_{1,2m_0,k}$ is complex.

Step 3. *Construction of adjoint modes.* Now we construct the adjoint modes $\mathbf{U}^{*1}$ and $\mathbf{U}^{*2}$ orthogonal to $\mathbf{u}^1$ and $\mathbf{u}^2$. Let us denote the real and imaginary parts of the critical adjoint eigenvector by $\mathbf{u}^{*1} = \mathrm{Re}\,\mathbf{u}^*_{m_0,1}$ and $\mathbf{u}^{*2} = \mathrm{Im}\,\mathbf{u}^*_{m_0,1}$ and define

$$\mathbf{U}^{*1} = \frac{(\mathbf{u}^1,\mathbf{u}^{*1})\mathbf{u}^{*1} + (\mathbf{u}^1,\mathbf{u}^{*2})\mathbf{u}^{*2}}{(\mathbf{u}^1,\mathbf{u}^{*1})^2 + (\mathbf{u}^1,\mathbf{u}^{*2})^2}, \quad \mathbf{U}^{*2} = \frac{-(\mathbf{u}^1,\mathbf{u}^{*2})\mathbf{u}^{*1} + (\mathbf{u}^1,\mathbf{u}^{*1})\mathbf{u}^{*2}}{(\mathbf{u}^1,\mathbf{u}^{*1})^2 + (\mathbf{u}^1,\mathbf{u}^{*2})^2}. \tag{2.24}$$

Noting that for any two functions of the form $f_i(x,y) = e^{iam\pi x}g_i(y)$ for $i = 1,2$, where m is a nonzero integer, we have

$$(\mathrm{Re}\,f_1, \mathrm{Re}\,f_2) = (\mathrm{Im}\,f_1, \mathrm{Im}\,f_2), \quad (\mathrm{Re}\,f_1, \mathrm{Im}\,f_2) = -(\mathrm{Im}\,f_1, \mathrm{Re}\,f_2).$$

Thus

$$(\mathbf{u}^1,\mathbf{u}^{*1}) = (\mathbf{u}^2,\mathbf{u}^{*2}), \quad (\mathbf{u}^1,\mathbf{u}^{*2}) = -(\mathbf{u}^2,\mathbf{u}^{*1}).$$

This implies that

$$\begin{aligned}
(\mathbf{u}^2,\mathbf{U}^{*1}) &= (\mathbf{u}^1,\mathbf{U}^{*2}) = 0,\\
(\mathbf{u}^1,\mathbf{U}^{*1}) &= (\mathbf{u}^2,\mathbf{U}^{*2}) = 1.
\end{aligned} \tag{2.25}$$

Step 4. *Derivation of the reduced equations.* Now we write

$$\mathbf{u}(x,y,t) = x_1(t)\mathbf{u}^1(x,y) + x_2(t)\mathbf{u}^2(x,y) + \Phi(x,y,t), \tag{2.26}$$

where Φ is the center manifold function, $x_1, x_2 \in \mathbb{R}$. Note that

$$L(\mathbf{u}^1 + i\mathbf{u}^2) = \beta(\mathbf{u}^1 + i\mathbf{u}^2)$$

amounts to saying that

$$L\mathbf{u}^1 = \mathrm{Re}(\beta)\mathbf{u}^1 - \mathrm{Im}(\beta)\mathbf{u}^2, \qquad L\mathbf{u}^2 = \mathrm{Re}(\beta)\mathbf{u}^2 + \mathrm{Im}(\beta)\mathbf{u}^1.$$

Also by definition of the center manifold, we have $(\Phi,\mathbf{u}^{*1}) = 0$ and $(\Phi,\mathbf{u}^{*2}) = 0$, which by (2.24) implies that

$$(\Phi,\mathbf{U}^{*i}) = 0, \qquad i = 1,2. \tag{2.27}$$

Hence by (2.25) and (2.27)

$$\begin{aligned}(L\mathbf{u},\mathbf{U}^{*1}) &= (x_1 L\mathbf{u}^1,\mathbf{U}^{*1}) + (x_2 L\mathbf{u}^2,\mathbf{U}^{*1}) = \mathrm{Re}(\beta)x_1 + \mathrm{Im}(\beta)x_2,\\ (L\mathbf{u},\mathbf{U}^{*2}) &= (x_1 L\mathbf{u}^1,\mathbf{U}^{*2}) + (x_2 L\mathbf{u}^2,\mathbf{U}^{*2}) = \mathrm{Im}(\beta)x_1 + \mathrm{Re}(\beta)x_2.\end{aligned} \tag{2.28}$$

Plugging (2.26) into (2.3), taking the inner product with $\mathbf{U}^{*i}$ $(i = 1, 2)$, and using (2.25) and (2.28), we can write the reduced equations as

$$\begin{aligned}\frac{dx_1}{dt} &= \mathrm{Re}(\beta)x_1 + \mathrm{Im}(\beta)x_2 + (G(\mathbf{u},\mathbf{u}),\mathbf{U}^{*1}),\\ \frac{dx_2}{dt} &= -\mathrm{Im}(\beta)x_1 + \mathrm{Re}(\beta)x_2 + (G(\mathbf{u},\mathbf{u}),\mathbf{U}^{*2}).\end{aligned} \tag{2.29}$$

Noting that

$$\begin{aligned}&G_s(\mathbf{u}^i,\mathbf{u}^j,\mathbf{U}^{*k}) = 0, \quad i,j,k = 1,2,\\ &G_s(\Phi,\Phi,\mathbf{U}^{*k}) = o(3),\end{aligned}$$

we can expand the nonlinear terms of x_1 and x_2 in (2.29):

$$(G(\mathbf{u},\mathbf{u}),\mathbf{U}^{*j}) = x_1 G_s(\mathbf{u}^1,\Phi,\mathbf{U}^{*j}) + x_2 G_s(\mathbf{u}^2,\Phi,\mathbf{U}^{*j}) + o(3). \tag{2.30}$$

By (2.23),

$$G_s(\mathbf{u}^i,\Phi,\mathbf{U}^{*j}) = \sum_k \Phi_{1,0k}(x_1^2 + x_2^2)c_{0k}^{ij} + \Phi_{1,2m_0,k}(x_1^2 - 2ix_1x_2 - x_2^2)c_{2m_0,k}^{ij}, \tag{2.31}$$

where we define

$$\begin{aligned}c_{0,k}^{ij} &= G_s(\mathbf{u}^i,\mathbf{u}_{0k},\mathbf{U}^{*j}),\\ c_{2m_0,k}^{ij} &= G_s(\mathbf{u}^i,\mathbf{u}_{2m_0,k},\mathbf{U}^{*j}).\end{aligned} \tag{2.32}$$

As in (2.17), we can show that

$$\begin{aligned}&c_{0k}^{11} = c_{0k}^{22}, && c_{0k}^{12} = -c_{0k}^{21},\\ &c_{2m_0,k}^{11} = -c_{2m_0,k}^{22}, && c_{2m_0,k}^{12} = c_{2m_0,k}^{21}.\end{aligned} \tag{2.33}$$

Moreover, the calculation

$$\begin{aligned}G_s(\mathbf{u}^1,\mathbf{u}_{2m_0}^1,\mathbf{U}^{*1}) &= G_s(\mathbf{u}^1,\mathbf{u}_{2m_0}^2,\mathbf{U}^{*2}),\\ G_s(\mathbf{u}^1,\mathbf{u}_{2m_0}^2,\mathbf{U}^{*1}) &= -G_s(\mathbf{u}^1,\mathbf{u}_{2m_0}^1,\mathbf{U}^{*2})\end{aligned} \tag{2.34}$$

implies that

$$c_{2m_0,k}^{11} = -ic_{2m_0,k}^{12}. \tag{2.35}$$

Using (2.30)–(2.35), we have

$$(G(\mathbf{u},\mathbf{u}),\mathbf{U}^{*j}) = b_{30}^j x_1^3 + b_{21}^j x_1^2 x_2 + b_{12}^j x_1 x_2^2 + b_{03}^j x_2^3 + o(3), \quad j = 1,2,$$

where simple calculations show that

$$\begin{aligned}b_{30}^1 = b_{12}^1 = b_{21}^2 = b_{03}^2 &= \sum_k \Phi_{1,0k}c_{0k}^{11} + \Phi_{1,2m_0,k}c_{2m_0,k}^{11},\\ b_{30}^2 = b_{12}^2 = -b_{21}^1 = -b_{03}^1 &= \sum_k \Phi_{1,0k}c_{0k}^{12} + i\Phi_{1,2m_0,k}c_{2m_0,k}^{11}.\end{aligned} \tag{2.36}$$

Thus the reduced equations (2.29) become

$$\begin{aligned}\frac{dx_1}{dt} &= \mathrm{Re}(\beta)x_1 + \mathrm{Im}(\beta)x_2 + b^1_{30}x_1(x_1^2+x_2^2) - b^2_{30}x_2(x_1^2+x_2^2) + o(3),\\ \frac{dx_2}{dt} &= -\mathrm{Im}(\beta)x_1 + \mathrm{Re}(\beta)x_2 + b^2_{30}x_1(x_1^2+x_2^2) + b^1_{30}x_2(x_1^2+x_2^2) + o(3).\end{aligned} \tag{2.37}$$

Step 5. *Computation of the transition number* γ. Letting $z = x_1 + ix_2$, (2.37) becomes

$$\frac{dz}{dt} = \overline{\beta}z + bz|z|^2 + o(|z|^3), \tag{2.38}$$

where by (2.35) and (2.36)

$$b = b^1_{30} + ib^2_{30} = \sum_k \Phi_{1,0k}(c^{11}_{0k} + ic^{12}_{0k}). \tag{2.39}$$

If $\mathrm{Re}\, b < 0$, then (2.38) has a stable limit cycle

$$z = re^{i\omega t}$$

for $\mathrm{Re}\,\beta > 0$, i.e., for $R > R_0$ with

$$r = \sqrt{-\frac{\mathrm{Re}\,\beta}{\mathrm{Re}\, b}}, \quad \omega = -\,\mathrm{Im}\,\beta + \mathrm{Im}\, br^2 = -\,\mathrm{Im}\,\beta + O(|\,\mathrm{Re}(\beta)|).$$

If $\mathrm{Re}\, b > 0$, then (2.38) has an unstable limit cycle for $R < R_0$.

Thus the transition is determined by the sign of the real part of b in (2.39) at $R = R_0$ defined as

$$\gamma = \mathrm{Re}(b) = \sum_{k=1}^{\infty} \Phi_{1,0k} c^{11}_{0k}, \tag{2.40}$$

since $\Phi_{1,0k}$, c^{11}_{0k}, c^{12}_{0k} are real numbers.

Step 6. *Derivation of the transition number* γ *in* (2.10). Using (2.18) in (2.22), we get

$$\Phi_{1,0k} = \frac{g^{11}_{0k}}{-\beta_{0k}(\mathbf{u}_{0k}, \mathbf{u}^*_{0k})}. \tag{2.41}$$

The mode $\mathbf{u}_{0k} = \mathbf{u}^*_{0k} = (\frac{\partial}{\partial y}\psi_{0k}, 0) = (DY_{0k}, 0)$ corresponds to the eigenfunction with $m = 0$ in (2.6), i.e., solutions of $ED^4Y = \beta D^2Y$ with the boundary conditions $Y(\pm 1) = D^2Y(\pm 1) = 0$. These solutions are easily obtainable.

$$\begin{aligned}\beta_{0k} &= -\frac{k^2\pi^2}{4}E,\\ Y_{0k} &= \begin{cases}\cos\frac{k\pi y}{2} & \text{if k is odd,}\\ \sin\frac{k\pi y}{2} & \text{if k is even.}\end{cases}\end{aligned} \tag{2.42}$$

Thus

$$(\mathbf{u}_{0k}, \mathbf{u}^*_{0k}) = \frac{2}{a}\int_{-1}^{1} |DY_{0k}|^2 = \frac{-2\beta_{0k}}{aE}.$$

To obtain γ, we need to compute

$$c_{0,k}^{11} = G_s(\mathbf{u}^1, \mathbf{u}_{0k}, \mathbf{U}^{*1}) = G(\mathbf{u}^1, \mathbf{u}_{0k}, \mathbf{U}^{*1}) + G(\mathbf{u}_{0k}, \mathbf{u}^1, \mathbf{U}^{*1}), \tag{2.43}$$

$$g_{0k}^{11} = G(\mathbf{u}^1, \mathbf{u}^1, \mathbf{u}_{0k}^*), \tag{2.44}$$

where $\mathbf{u}^1$ is the real part of the critical eigenfunction (with zonal wavenumber m_0) as given in (2.12), $\mathbf{U}^{*1}$ is given by (2.24), and G is the trilinear operator (2.13). So we plug $\psi_{m_0 1} = e^{iam_0\pi x} Y_{m_0 1}(y)$ and $\psi_{m_0 1}^* = e^{iam_0\pi x} Y_{m_0 1}^*(y)$ into (2.43) and (2.44). After tedious computations, we can obtain

$$\begin{aligned} c_{0k}^{11} &= -\frac{a\epsilon m_0 \pi}{|J_1|^2} \operatorname{Im}\{J_1 J_2(k)\}, \\ g_{0k}^{11} &= -\frac{\epsilon m_0 \pi \beta_{0k}}{E} \operatorname{Im} J_3(k), \end{aligned} \tag{2.45}$$

where

$$\begin{aligned} J_1 &= \int_{-1}^{1} \overline{Y^*}((am_0\pi)^2 - D^2) Y \, dy, \\ J_2(k) &= \int_{-1}^{1} D Y_{0k} \overline{Y^*} \left((am_0\pi)^2 - \frac{k^2\pi^2}{4} - D^2 \right) Y \, dy, \\ J_3(k) &= \int_{-1}^{1} Y_{0k} Y D\overline{Y} \, dy. \end{aligned} \tag{2.46}$$

Finally, we note that $Y = Y_{m_0 1}$ is either an odd or an even function of y which follows from the fact that (2.6) is invariant under the change of variables $y \to -y$. Thus by (2.42), Y_{0k} must be odd and k must be even; otherwise $J_3(k)$ is zero. Hence the nonzero contributions to γ in (2.40) come from even k. Thus we obtain the specific form of γ given by (2.10), from (2.40), (2.41), (2.42), (2.45), and (2.46).

Finally, the stability and transition behavior follows from the general framework in [11, Theorem 2.3.7]. The proof is then complete. ∎

3. Numerical evaluation. Theorem 2.1 offers the precise information on the type of transitions and stability of the bifurcation periodic solutions of the basic flow, fully dictated by the nondimensional parameter $\gamma = \gamma(a, \epsilon, E)$ given in (2.10). Equation (1.5) defines a hypersurface in the physical parameter space, leading to the phase transition diagram in terms of the physical parameters: the length scale a, the Rossby number ϵ, and the Ekman number E.

We explore in this section the dynamic transition behavior of the basic flow in different physical parameter regimes by combining the rigorous analytic results, obtained in Theorem 2.1, with numerical computation. It is worth noting that as the type of transitions and stability of the bifurcation periodic solutions of the basic flow are completely dictated by sign of the parameter $\gamma = \gamma(a, \epsilon, E)$ given in (2.10), the definite physical conclusions can be derived through the combination of rigorous analysis and robust numerical computation as performed in this section.

3.1. Legendre–Galerkin method for (2.6) and (2.7). In this section we present a method to approximate the solutions of the eigenvalue problems (2.6) and (2.7). These are both fourth-order problems, so a Legendre–Galerkin method [15, 16] will be efficient and accurate.

We look for an approximation of Y in the space $X_N = \{v \in P_N : v(\pm 1) = v''(\pm 1) = 0\}$, where P_N is the space of polynomials with degree less than or equal to N.

Using the approach in [15], we set

$$f_j(y) = L_j(y) + \sum_{k=1}^{4} c_{j,k} L_{j+k}(y),$$

with $c_{j,k}$ to be chosen such that

$$f_j(\pm 1) = f_j''(\pm 1) = 0.$$

It is easy to determine from the properties of Legendre polynomials that

$$\begin{aligned} c_{j,1} &= c_{j,3} = 0, \\ c_{j,2} &= \frac{2(2j+5)(j^2+5j+9)}{(j+3)(j+4)(2j+7)}, \\ c_{j,4} &= -1 - c_{j,2}, \end{aligned}$$

and we have $X_N = \operatorname{span}\{f_j : j = 0, 1, \ldots, N-4\}$.

Writing $Y^N(y) = \sum_{j=0}^{N-4} y_j f_j(y) \in X_N$, plugging it into (2.6), and taking the inner product with $f_k(y)$ $(k = 0, 1, \ldots, N-4)$, we obtain the Legendre–Galerkin approximation of (2.6) in the following matrix form:

$$\begin{aligned} &\left(E(A_1 - 2\alpha_m^2 A_2 + \alpha_m^4 A_3) + i\alpha_m \left(\frac{R}{\pi^3} A_4^T + \frac{R}{\pi^3}(\pi^2 - \alpha_m^2) A_5 - A_3 \right) \right) \mathcal{Y}^N \\ &= \beta (A_2 - \alpha_m^2 A_3) \mathcal{Y}^N, \end{aligned} \tag{3.1}$$

where

$$\begin{aligned} A_i &= (a_{i,jk})_{j,k=0,\ldots,N-4} \qquad \text{for } i = 1, \ldots, 5, \\ \mathcal{Y}^N &= \begin{bmatrix} y_0 & y_1 & \cdots & y_{N-4} \end{bmatrix}^T. \end{aligned}$$

Here

$$\begin{aligned} &a_{1,jk} = (D^4 f_j, f_k), && a_{2,jk} = (D^2 f_j, f_k), && a_{3,jk} = (f_j, f_k), \\ &a_{4,jk} = (\cos \pi y \, D^2 f_j, f_k), && a_{5,jk} = (\cos \pi y \, f_j, f_k). \end{aligned}$$

By using the properties of Legendre polynomials, we find that A_1, A_2, A_3 are real symmetric banded matrices given by

$$a_{1,jk} = \begin{cases} \dfrac{(2+2j)(2+j)(3+2j)^2(5+2j)}{(3+j)(4+j)} & \text{if } j = k, \\ 0 & \text{otherwise,} \end{cases}$$

$$a_{2,jk} = \begin{cases} \dfrac{(2+2j)(2+j)(3+2j)}{(3+j)(4+j)} & \text{if } j = k \pm 2, \\ \dfrac{4(3+2j)(5+2j)(102+110j+47j^2+10j^3+j^4)}{(3+j)^2(4+j)^2(7+2j)} & \text{if } j = k, \\ 0 & \text{otherwise,} \end{cases}$$

$$a_{3,jk} = \begin{cases} \dfrac{2(1+j)(2+j)(3+2j)}{(3+j)(4+j)(7+2j)(9+2j)} & \text{if } j = k \pm 4, \\ \dfrac{-8(222+196j+77j^2+14j^3+j^4)}{(3+j)(4+j)(5+j)(6+j)(11+2j)} & \text{if } j = k \pm 2, \\ \dfrac{4(5580+11202j+9263j^2+4170j^3+1105j^4+168j^5+12j^6)}{(3+j)^2(4+j)^2(1+2j)(7+2j)(9+2j)} & \text{if } j = k, \\ 0 & \text{otherwise.} \end{cases}$$

To approximate A_4 and A_5 we fix some integer M and compute the Legendre–Gauss–Lobatto quadrature points y_n and weights ω_n for $n = 0, \dots, M$. Then we compute the matrices $D^2 f_j(y_n)$ and $f_j(y_n)$ as follows:

$$a_{4,jk} = \sum_{n=0}^{M} \cos(\pi y) D^2 f_j(y_n) f_k(y_n) \omega_n,$$
$$a_{5,jk} = \sum_{n=0}^{M} \cos(\pi y) f_j(y_n) f_k(y_n) \omega_n.$$

The integer M is chosen large enough to provide sufficient accuracy in the computation of A_4 and A_5. We note that A_4 and A_5 are real, full matrices and that A_5 is symmetric while A_4 is nonsymmetric.

The eigenvalue problem (3.1) can be easily solved by using a standard eigenvalue solver. For each $m \in \mathbb{Z}$, we can numerically find the $N-3$ eigenvalues $\beta_{m,j}^N$ (with $\operatorname{Re}\beta_{m,j}^N \geq \operatorname{Re}\beta_{m,k}^N$ if $j < k$) of (3.1) and the corresponding eigenvectors $\mathcal{Y}_{m,j}^N$, $j = 1, \dots, N-3$.

By taking the complex conjugate of (3.1), we find that $\mathcal{Y}_{m,j}^N = \overline{\mathcal{Y}}_{-m,j}^N$, $\beta_{m,j}^N = \overline{\beta}_{-m,j}^N$, and in particular β_{0j}^N and ψ_{0j}^N are real.

It is known [17] that the computed eigenpairs $(\beta_{m,j}^N, e^{i\alpha_m x} Y_{m,j}^N)$ of (3.1) converge to eigenpairs $(\beta_{m,j}, \psi_{m,j})$ of (2.4) exponentially as $N \to \infty$ for $0 \leq j \lesssim 2N/\pi$ for each fixed m.

Finally, the analogue of approximating (3.1) for the adjoint problem (2.7) is the adjoint problem of (3.1). Namely.

$$\left(E(A_1 - 2\alpha_m^2 A_2 + \alpha_m^4 A_3) - i\alpha_m \left(\frac{R}{\pi^3} A_4 + \frac{R}{\pi^3}(\pi^2 - \alpha_m^2) A_5 - A_3 \right) \right) \mathcal{Y}^{*N} = \beta^* (A_2 - \alpha_m^2 A_3) \mathcal{Y}^{*N}. \tag{3.2}$$

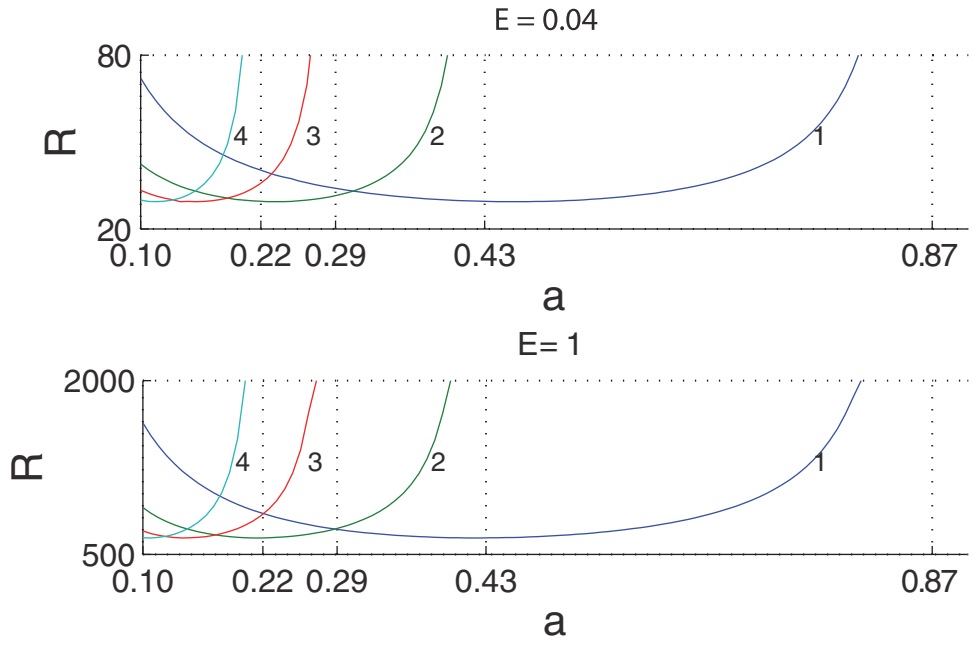

FIG. 1. *Neutral stability curves which are defined by* $\mathrm{Re}\,\beta_{m,1} = 0$ *in the* a*-*R *plane for zonal wavenumbers* $m = 1, 2, 3, 4$ *and for* $E = 0.04$, $E = 1$.

3.2. Numerical computation of the transition number γ. To approximate γ in (2.10), we proceed in the following steps:

Step 1. The parameters of the system are a, ϵ, E, and R. We fix the Ekman number E and the length scale a. Then by (1.2), the Rossby number $\epsilon = R/E$ is also fixed. Moreover, to study the transition, R has to be fixed to $R = R_0$, where R_0 is determined by Assumption 1.

Step 2. We determine the critical zonal wavenumber m_0 and the critical Reynolds number R_0 in Assumption 1. In [3], it was shown that $m_0 = 1$ if $\sqrt{3}/4 \le a \le \alpha_0$ for some $\alpha_0 < \sqrt{3}/2$. Figure 1 shows that the difficulties in proving Assumption 1 for $\alpha_0 \le a < \sqrt{3}/2$ are purely technical. Extrapolating this result supported by our numerical computations of neutral stability curves shown in Figure 1, we claim that Assumption 1 can be satisfied by m only if $a < \sqrt{3}/(2m)$.

For such m, we set $\mathrm{Re}\,\beta^N_{m,1} = 0$ in (3.1) and solve for the Reynolds number R to find $R^N_{0,m}$. R^N_0, which approximates R_0, is the minimum of such $R^N_{0,m}$, and the minimizing m value is m_0.

Figure 1 shows that Assumption 1 holds for a simple complex pair of eigenvalues for almost all $a < \sqrt{3}/2$, except for discrete values of a where neutral stability curves corresponding to different zonal wavenumbers intersect; Assumption 1 is generic.

Step 3. With $\beta^N_{m_0,1}$ computed, the eigensolutions $\mathcal{Y}^N_{m_0,1} = [\tilde{y}_j]_{j=0}^{N-4}$ and $\mathcal{Y}^{*N}_{m_0,1} = [\tilde{y}^*_j]_{j=0}^{N-4}$ of (3.1) and (3.2) are also found.

Step 4. The Legendre–Gauss–Lobatto quadrature points y_j and weights ω_j are

calculated for $j = 0, \ldots, M$, where M is chosen large enough to allow sufficient accuracy in the computation of (3.3).

Step 5. The values of the eigenmodes and their derivatives at quadrature points y_j are computed.

$$Y^N_{m_0,1}(y_j) = \sum_{k=0}^{N-4} \tilde{y}_k f_k(y_j), \qquad Y^{*N}_{m_0,1}(y_j) = \sum_{k=0}^{N-4} \tilde{y}^*_k f_k(y_j),$$

$$DY^N_{m_0,1}(y_j) = \sum_{k=0}^{N-4} \tilde{y}_k f'_k(y_j), \qquad D^2Y^N_{m_0,1}(y_j) = \sum_{k=0}^{N-4} \tilde{y}_k f''_k(y_j).$$

Step 6. It is easy to see that if we multiply $Y_{m_0,1}$ by a complex number c, then γ is multiplied by $|c|^2$. To find a unique γ, we normalize $Y_{m_0,1}$ so that $\max_{0\le j\le M} Y^N_{m_0,1}(y_j) = 1$. We also normalize $Y^{*N}_{m_0,1}$ so that $I_1 = 1$ in (2.9). It is easy to see that this scaling has no effect on γ.

Step 7. Finally, we approximate $I_2(k)$, $I_3(k)$ by

(3.3)

$$I_2(k) \approx \sum_{j=0}^{M} \cos(k\pi y_j) Y^{*N}_{m_0,1}(y_j) \left((am_0\pi)^2 - k^2\pi^2 - D^2\right) \overline{Y^N_{m_0,1}(y_j)}\omega_j,$$

$$I_3(k) \approx \sum_{j=0}^{M} \sin(k\pi y_j) Y^N_{m_0,1}(y_j) \overline{DY^N_{m_0,1}(y_j)}\omega_j.$$

Obviously, increasing M increases the accuracy of approximation in (3.3). In our experiments we found that $M = 2N$ gives enough accuracy.

3.3. Numerical results. In this section, we present the results of our numerical computations of γ for different parameter choices. As discussed in section 3.2, the only parameters that need to be varied are the Ekman number E and the length scale a.

To illustrate the typical results, we consider a midlatitude atmospheric jet in a zonal channel at a reference latitude $\theta_0 = 45°$N. The dimensional zonal velocity of the background state u_0 in (1.4) has a maximum $U/(\pi^3 E)$. With a typical zonal velocity of $U = 15$ ms^{-1}, we limit our numerical investigations to E values between 0.01 and 0.03 that correspond to maximum zonal jet velocities between 16 ms^{-1} up to 48 ms^{-1}. For $a = 0.2$, a typical length scale of $L = 3000$ km yields a channel of length $2L/a = 30000$ km in the meridional direction that corresponds to about 360° in longitude. We therefore consider a values in the range $0.1 \le a \le 0.6$.

For this parameter regime we approximate the transition number γ following the procedure in section 3.2. The results we find are presented in Table 1, which suggest that γ is always positive. According to Theorem 2.1, this means that the transition is catastrophic (Type-II) at the first critical Reynolds number R_0.

We can also compute the period $T = 2\pi/\operatorname{Im}\beta_{m_0,1}$ of the solution (2.11), where T has been nondimensionalized by $1/(\beta_0 L)$. For example, with the above choices of L and U, for $a = 0.20$ and $E = 0.01$ we find that $m_0 = 2$, $R_0 = 5.64$. The planetary vorticity gradient β_0 at 45N is 1.6×10^{-11}. We compute the period to be about $T = 196$ days. The stream function of the time periodic solution (2.11) bifurcated on $R < R_0$, which is unstable because of the Type-II transition, is shown in Figure 2. The pattern indicates a typical one due to barotropic instability which, due to the background state zonal velocity, propagates eastward.

TABLE 1
The value of γ *for* $0.1 \le a \le 0.6$ *and* $0.01 \le E \le 0.03$.

		a					
		0.100	0.200	0.300	0.400	0.500	0.600
E	0.010	0.197	0.197	0.188	0.197	0.194	0.175
	0.015	0.174	0.174	0.163	0.174	0.172	0.155
	0.020	0.156	0.156	0.143	0.156	0.156	0.143
	0.025	0.144	0.144	0.130	0.144	0.146	0.135
	0.030	0.135	0.135	0.121	0.135	0.139	0.130

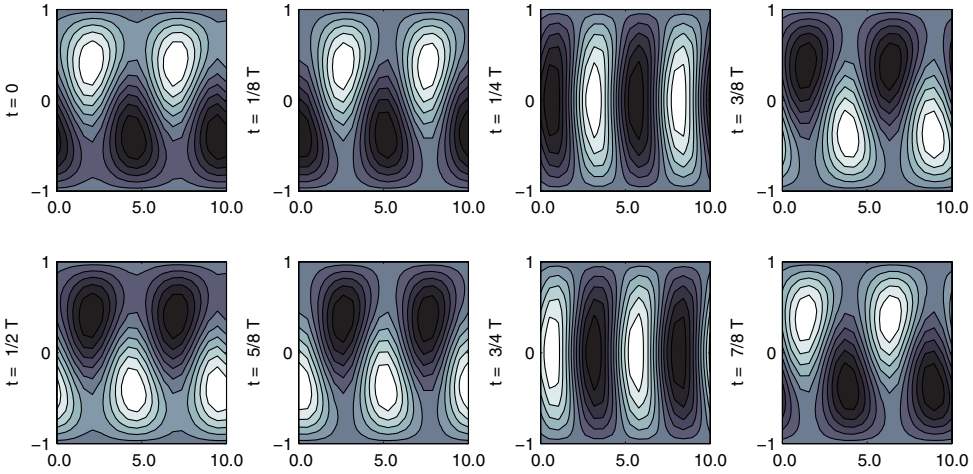

FIG. 2. *The stream function of the bifurcated periodic solution on* $R < R_0$ *at* $a = 0.2$ *and* $E = 0.01$*; T denotes the period of the periodic orbit.*

4. Summary and discussion. In this paper, we have extended the results of [3] on the existence of a Hopf bifurcation in the forced barotropic vorticity equation (1.1) by rigorously showing the type of finite amplitude solutions which can occur near this Hopf bifurcation. Central in the analysis is the computable quantity γ, which characterizes the transition behavior near the critical point.

The aim of this paper was only to focus on the theory and numerical computation. As an illustration, we explore this number numerically in a parameter regime relevant for an atmospheric jet and find that a catastrophic transition is preferred. For typical ocean cases, for example in western boundary currents such as the Gulf Stream and the Kuroshio, and the Antarctic Circumpolar Current, the results will be reported elsewhere.

While (1.1) is a cornerstone dynamical model of the ocean and atmospheric circulation, it of course represents only a limited number of processes. As practiced by the earlier workers in this field, such as J. Charney and J. von Neumann, and from the lessons learned by the failure of Richardson's pioneering work, one tries to be satisfied with simplified models approximating the actual motions to a greater or lesser degree instead of attempting to deal with the atmosphere/ocean in all its complexity. By

starting with models incorporating only what are thought to be the most important of atmospheric influences, and by gradually bringing in others, one is able to proceed inductively and thereby avoid the pitfalls inevitably encountered when a great many poorly understood factors are introduced all at once.

However, the same results will be true if we work on the barotropic equations in primitive variables; see (2.2) and [13]. Second, we expect that the same type of results obtained in this paper will also be true if we use higher-order friction (e.g. hyperfriction [14]) in (1.1), as this would only change the eigenfunction structure slightly. Third, the method presented in this paper combined with the methods introduced in [1, 2] can be used to study the case with bottom topography [4] and the case where noise represents ocean eddies. We will explore these new directions in the near future.

Acknowledgment. The authors are grateful for the insightful comments by the two anonymous referees.

REFERENCES

[1] M. Chekroun, H. Liu, and S. Wang, *Approximation of Invariant Manifolds: Stochastic Manifolds for Nonlinear SPDEs* I, Springer Briefs Math., Springer, New York, 2014.
[2] M. Chekroun, H. Liu, and S. Wang, *Parameterizing Manifolds and Non-Markovian Reduced Equations: Stochastic Manifolds for Nonlinear SPDEs* II, Springer Briefs Math., Springer, New York, 2014.
[3] Z.-M. Chen, M. Ghil, E. Simonnet, and S. Wang, *Hopf bifurcation in quasi-geostrophic channel flow*, SIAM J. Appl. Math., 64 (2003), pp. 343–368.
[4] D. T. Crommelin, J. D. Opsteegh, and F. Verhulst, *A mechanism for atmospheric regime transitions*, J. Atmospheric Sci., 61 (2004), p. 1406–1419.
[5] H. Dijkstra, *Nonlinear Climate Dynamics*, Cambridge University Press, Cambridge, UK, 2013.
[6] H. A. Dijkstra, *Nonlinear Physical Oceanography: A Dynamical Systems Approach to the Large Scale Ocean Circulation and El Niño*, Kluwer Academic Publishers, Dordrecht, The Netherlands, 2000.
[7] H. A. Dijkstra and M. Ghil, *Low-frequency variability of the large-scale ocean circulations: A dynamical systems approach*, Rev. Geophys., 43 (2005), pp. 1–38.
[8] M. Ghil, *Is our climate stable? Bifurcations, transitions and oscillations in climate dynamics*, in Science for Survival and Sustainable Development, V. I. Keilis-Borok and M. Sánchez Sorondo, eds., Pontifical Academy of Sciences, Vatican City, 2000, pp. 163–184.
[9] IPCC, 2013, *Climate Change* 2013: *The Physical Science Basis. Contribution of Working Group* I *to the Fifth Assessment Report of the Intergovernmental Panel on Climate Change (IPCC)*, T. F. Stocker et al., eds., Cambridge University Press, Cambridge, UK, New York, 2013; also available online from www.ipcc.ch.
[10] T. Ma and S. Wang, *Bifurcation Theory and Applications*, World Sci. Ser. Nonlinear Sci. Ser. A Monogr. Treatises 53, World Scientific Publishing, Hackensack, NJ, 2005.
[11] T. Ma and S. Wang, *Phase Transition Dynamics*, Springer-Verlag, New York, 2013.
[12] J. Pedlosky, *Geophysical Fluid Dynamics*, 2nd ed., Springer-Verlag, New York, 1987.
[13] T. Sapsis and H. A. Dijkstra, *Interaction of additive noise and nonlinear dynamics in the double-gyre wind-driven ocean circulation*, J. Phys. Oceanography, 43 (2013), pp. 366–381.
[14] F. M. Selten, *An efficient description of the dynamics of barotropic flow*, J. Atmospheric Sci., 52 (1995), pp. 915–936.
[15] J. Shen, *Efficient spectral-Galerkin method* I. *Direct solvers for second- and fourth-order equations using Legendre polynomials*, SIAM J. Sci. Comput., 15 (1994), pp. 1489–1505.
[16] J. Shen, T. Tang, and L.-L. Wang, *Spectral Methods: Algorithms, Analysis and Applications*, Springer Ser. Comput. Math. 41, Springer, Heidelberg, 2011.
[17] J. A. C. Weideman and L. N. Trefethen, *The eigenvalues of second-order spectral differentiation matrices*, SIAM J. Numer. Anal., 25 (1988), pp. 1279–1298.